Wheel-Load-Induced Earth Pressures on Box Culverts

RAY W. JAMES AND DALE E. BROWN

A full-scale 8- by 8-ft reinforced-concrete box culvert was constructed and instrumented with earth pressure cells. Dead loads caused by backfill and up to 8 ft of cover were applied in 2-ft increments. Live loads were applied at each level of cover by a test vehicle loaded to represent the alternate interstate design load, consisting of two 24,000-lb axles spaced 4 ft apart. Measured live-load earth pressures on the top slab are compared to various theoretical solutions for concentrated and distributed wheel loads and to pressures predicted by a finite element model. Empirical equations are presented that for shallow covers more accurately model the measured data than do the analytical and numerical methods studied.

The prediction of live-load-induced earth pressures on culverts under shallow fill is accomplished in design by empirical methods such as the AASHTO pyramid loading (*1*), in which the vertical pressure caused by a concentrated or distributed load on the surface is calculated by dividing the load by the area of the base of a four-sided pyramid having sides with specified slopes and apex at the location of the concentrated load or truncated top at the rectangular distributed surface load. Applicable theoretical methods (*2-5*) are generally based on elasticity solutions, usually involving simplifying assumptions of linearly elastic, isotropic behavior. In addition, such methods are cumbersome for application in design. Finite element methods using such programs as CANDE (*6*) and SST1PN (a code written at the University of California at Berkeley) have become widely used in design for prediction of earth pressures accounting for nonlinear material behavior, soil-structure interaction, and complex geometries that cannot be easily modeled with the analytical methods. Essential to any finite element model are data for testing the validity of assumptions regarding material properties and soil-structure interaction mechanisms. Anand (*7*) describes the need for reliable full-scale model data as follows: "Most of all, experimental data from full-scale models of shallow buried rigid pipes are desperately needed to verify the proposed analysis." While some recent data (*8*) have been developed concerning blast loading of concrete structures under shallow earth covers, few data for wheel-load-induced pressures have been reported.

R. W. James, Department of Civil Engineering, Texas A&M University, College Station, Tex. 77843-3136. D. E. Brown, Engineering Department, Chandler, Ariz. 85224.

DESCRIPTION OF EXPERIMENT

Culvert and Instrumentation

An 8- by 8- by 44-ft-long (2.44- by 2.44- by 13.41-m) reinforced-concrete box culvert was constructed in February 1982. Thicknesses of the side walls and slabs were 8 in. (20.3 cm) and 7 in. (17.8 cm), respectively. The culvert was constructed according to current Texas SDHPT standard specifications for SC-NB Type 3 single culverts—normal. The selected 44-ft (13.41-m) length was designed to allow construction of a 12-ft (3.66-m) roadway with 2:1 side slopes across the culvert. Twelve Terra Technology Model T-9010 total pressure cells were installed in the top slab flush with the top surface at locations described in Figure 1. The pressure cells had a full-scale range of 250 psi (1,720 kPa) and a manufacturer's specified accuracy of 0.1 percent full scale. The readings were taken with a 50-psi (7.3-kPa) full-scale pressure gauge and a resolution of 0.1 psi (0.7 kPa). Other instrumentation included pressure cells on the side walls and resistance strain gauges bonded to the reinforcing steel of the top slab. Measurements of top-slab deflection were made with a deflection dial gauge. The top-slab pressure cells were arranged in two banks of six cells each. The pressure cells

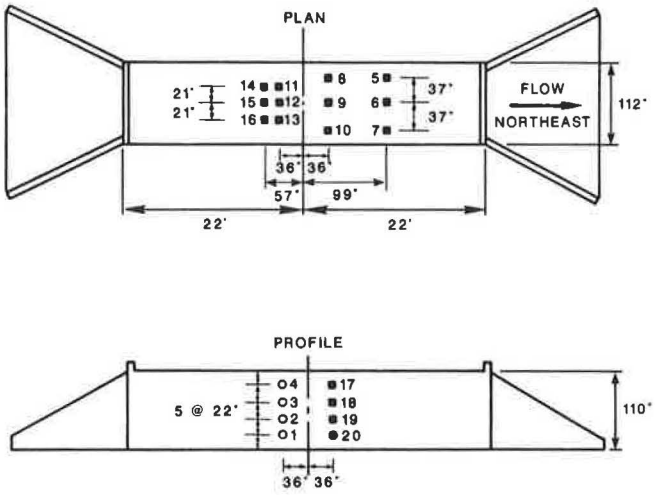

FIGURE 1 Test culvert and instrumentation.

used were static devices, incapable of indicating dynamic loads.

During February 1982 through September 1984, backfill and cover were placed, and measurements of dead- and live-load-induced earth pressures and strains in reinforcing steel were made. The measured live-load pressures on the top slab are presented herein. Live loads were applied by parking a test vehicle at a designated location above the culvert, and recording the static earth pressures applied to the culverts. Testing was repeated at various cover depths from 8 in. (20.3 cm) to 8 ft (2.44 m). The soil used to backfill and to cover the culvert was obtained at the test site, and has been classified as SC-SP, according to the Unified Soil Classification System. The liquid limit and plasticity index were 37.5 and 21.3 percent, respectively. The effective stress parameters C and ϕ were 0 and 31.8°, respectively. The soil properties and construction sequence are described in detail by James et al. (*9*).

Test Procedure

The test vehicle was a five-axle tractor-semitrailer combination vehicle, having the geometry and axle weights shown in Figure 2. The test vehicle essentially simulated the alternate interstate design load, a tandem of two 24-kip (107-kN) axles spaced 4 ft (1.22 m) apart. The effects of the lightly loaded tractor tandem and the steering axle were observed to be insignificant in comparison to the effect of the heavily loaded rear tandem.

The test vehicle was parked with the loaded tandem in various locations, as presented in Table 1. The pressure cells were pressurized according to the manufacturer's specifications, and the indicated pressures recorded. Three separate readings were taken for averaging, unless the first two readings were in agreement within 0.1 psi (0.7 kPa).

Data Reduction and Presentation

The recorded data were reduced and plotted using a microcomputer. Data reduction consisted of subtracting the indicated pressure with no live load applied from the indicated pressure with live load applied. No temperature correction

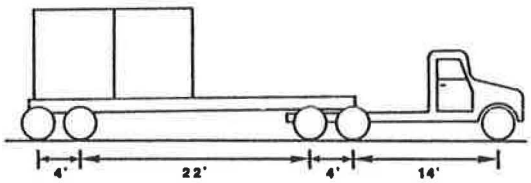

APRIL 1983					
LEFT SIDE	11,600	11,720	3,810	4,100	4,500
RIGHT SIDE	12,340	12,770	3,930	4,170	4,500
TOTAL	24,140	24,490	7,740	8,270	9,000
JUNE 1984					
LEFT SIDE	11,480	11,300			
RIGHT SIDE	12,980	12,870	NO DATA TAKEN		NO DATA TAKEN
TOTAL	24,430	24,250			

FIGURE 2 Test vehicle geometry and axle weights.

was required because the only observed effect of temperature on the cells was a change in the zero pressure offset. The effect of this variable offset was eliminated by subtracting the indicated pressure for the dead load as long as the temperature of the cell did not change between the two measurements. Because indicated pressures for the dead load were usually measured immediately before application of the live load, this temperature requirement was satisfied. The dead-load pressures, discussed by James et al. (*9*), did indicate a significant dependence on temperature, attributed to differential thermal expansion of the culvert and soil system.

MEASURED EARTH PRESSURES

The measured live-load earth pressures are presented in Table 1.

EMPIRICAL PRESSURE PREDICTION EQUATIONS

A number of functions were fit to the data of Table 1 in an attempt to develop an empirical equation for use in predicting design pressures under shallow covers. Existing theoretical equations for concentrated loads on the surface, such as Boussinesq's equation and Westergaard's equation, are not applicable for depths of cover that are not significantly greater than some characteristic dimension of the loaded area (*10*). In addition, these theoretical equations are based on a linearly elastic behavior within the soil, and the validity of this simplification is not certain. However, these equations were included in the set of candidate functions.

$$P_{VL} = W_i F(r, z) \quad (1)$$

where

P_{VL} = live-load vertical pressure,
W_i = wheel load, and
$F(r, z)$ = reciprocal area that depends on radial distance r and vertical distance z.

The functions considered included the following:

$$F(r, z) = (1.5/\pi)(Az)^3[(Br)^2 + (Az)^2]^{-2.5} \quad (2a)$$

$$F(r, z) = [\pi(Az)^2]^{-1}[1 + 2(Br/Az)^2]^{-1.5} \quad (2b)$$

$$F(r, z) = (\pi r_0^2)^{-1} \exp(-z/z_0)\exp\{-[\exp(-z/z_0)](r/r_0)^2\} \quad (2c)$$

and several members of the family

$$F(r, z) = \exp[-(Br/r_0)^2] \quad (2d)$$

including functions $r_0(z)$ such as

$$r_0(z) = (z/z_0) \quad (2e)$$

$$r_0(z) = (z/z_0)^{0.5} \quad (2f)$$

$$r_0(z) = \exp[(z/z_0)^2] \quad (2g)$$

$$r_0(z) = \exp(0.5z/z_0) \quad (2h)$$

Equation 2a is a form of Boussinesq's equation, as adapted to soils engineering by Jurgenson (*3*) and here modified by the dimensionless parameters A and B that multiply the z and r position variables, respectively. Equation 2b is a form of Westergaard's equation (*11*), modified here by the dimensionless parameters A and B. Equation 2c is an empirical equation that satisfies equilibrium and appropriate boundary conditions and that has been suggested as a model of the vertical live-load earth pressures (*9*). The parameters z_0 and r_0 are constant characteristic lengths that can be determined to best fit the data. Equation 2d is a family of functions that also satisfy equilibrium and the appropriate boundary conditions, but that are expressed in terms of a constant length parameter z_0 and a function $r_0(z)$ that depends on the dimensionless variable z/z_0. Functions $r_0(z)$ that were considered are listed in Equations 2e through 2h.

These theories do not include the effect of soil-structure interaction, and are therefore expected to predict pressures slightly greater than the actual pressures.

Regression Method

The best-fit parameters A, B, r_0, and z_0 for the equations listed were determined approximately by nonlinear regression. The error norm minimized was

$$\left|(P_t - P_m)\exp(-r/0.5)\right|$$

where P_t and P_m were theoretical and measured earth pressures, respectively.

The weighted error norm was calculated for the various equations and local minimums were identified. The weighting function was arbitrarily chosen so that pressures near points beneath an applied load were more heavily weighted than pressures at points some horizontal distance from an applied load. The corresponding values of the parameters and the ranges checked are presented in Table 2.

Discussion of Results

The results of the regression analysis are presented in Figures 3-11, which show the predicted pressures along a wheel path for each of the equations evaluated. The pressures indicated for the six pressure cells along either wheel path are presented for comparison. The earth pressures predicted from Equations 2e through 2h are not presented because the regression analysis results in Table 2 indicate relatively poor fits. Also shown for comparison are curves representing Boussinesq's equation integrated over four uniformly loaded 10- by 20-in. (25.4- by 50.8-cm) AASHTO footprints. No parameters were introduced to fit these curves to the data.

The Boussinesq equation (2a) and the Westergaard equation (2b) are shown as nearly identical curves, as expected. For shallow covers however, these two equations greatly overestimate the peak pressure directly beneath the wheel footprint. Because both equations are based on theories of earth pressure beneath concentrated loads, this observation is not unexpected. Because the maximum earth pressure beneath a wheel is limited to pressures not much more than the tire pressure, which is approximately 70 psi (482 kPa), the predicted pressures of over 170 psi (1,160 kPa) at 8-in. (20.3-

TABLE 1 MEASURED EARTH PRESSURES

EARTH COVER in feet	LOAD LOC. in feet	MEASURED EARTH PRESSURE IN PSI CELL NO. 5	6	7	8	9	10	11	12	13	14	15	16
(1)	(2)	(3)	(4)	(5)	(6)	(7)	(8)	(9)	(10)	(11)	(12)	(13)	(14)
1	0.0	0.2	0.3	-0.1	-0.3	-0.1	3.9	34.1	-0.1	17.4	0.1	-0.6	-0.3
2	3.0	0.1	-0.2	0.0	0.0	7.4	3.1	0.3	5.7	6.2	-0.2	3.4	3.0
2	-4.7	0.1	0.0	0.0	0.1	0.0	11.1	0.3	0.1	7.5	0.0	-0.5	2.3
2	0.0	0.1	-0.1	0.4	7.1	2.5	6.0	13.2	2.1	11.6	2.2	0.0	3.5
2	4.7	0.1	0.0	0.5	10.5	0.0	0.0	8.5	0.6	0.2	1.8	-0.4	-0.2
4	0.0	0.2	-0.2	0.1	3.3	1.5	2.9	4.1	1.5	2.2	1.8	1.6	2.1
4	3.0	-0.2	-0.4	0.0	3.5	0.6	0.3	3.3	1.1	-0.1	1.4	0.7	0.1
6	0.0	-0.2	-0.4	0.2	1.2	0.5	1.2	1.9	0.5	0.7	0.8	0.5	0.7
8	0.0	0.7	0.0	0.6	1.9	0.9	1.6	1.7	0.6	1.3	0.7	0.8	0.9

Note: Load location is the distance from the culvert centerline, measured along the perpendicular roadway centerline to the center of the loaded tandem. The axle spacing is 4 ft and the tread width is approximately 6.33 ft. The tandem is centered with respect to the roadway centerline.

cm) cover are clearly erroneous. The peak pressure predicted by Equation 2c is in much better agreement with the measured pressures and the upper bound approximated by the tire pressure. The curve corresponding to the empirical Equation 2c fits the measured data at 2 ft better than the Boussinesq and Westergaard theories, although the qualitative fit of all three curves to the data at this cover depth is judged to be acceptable. The Boussinesq equation applied to the uniformly loaded AASHTO footprints fits the data much better than the simpler equations corresponding to concentrated loads; however, the derivations from the measured pressures are consistently unconservative, in spite of the expected conservative deviation due to the neglect of soil-structure interaction. The proposed Equation 2c fits the data better, and deviations would result in conservative designs.

Also shown in Figure 6 is a comparison to a pretest two-dimensional prediction of live-load pressure distribution over the top slab for an equivalent live-load distribution (*13*). Although direct comparison of the numerical solution to measurements is hampered by the difference in modeled and actual loadings, it can be seen that the SSTIPN finite element solution obtained in this instance results in unconservative pressures on the top slab. The assumptions in the method of distributing wheel loads along the length of the structure are thought to be conservative; however, the resulting predicted earth pressures are unconservative. A similar comparison is shown in Figure 8 for 4-ft (1.22-m) cover. The finite element solution for this cover depth more closely approximates the measured data, when the difference in the loadings is taken into consideration.

At depths of cover equal to or exceeding 4 ft (1.22 m), the Boussinesq and Westergaard equations (2a and 2b) fit the data better than Equation 2c. The differences in predicted and measured pressures are slight for all three equations; however, the data indicate locally higher pressures beneath each wheel, as predicted by the Boussinesq and Westergaard theories for depths as great as 8 ft (2.44 m). The curve corresponding to Equation 2c predicts a single local maximum pressure along the wheel path for depths of 4 ft (1.22 m) or more. The Boussinesq equations for uniformly loaded AASHTO footprints again are consistently unconservative compared to the measured pressures.

Several factors account for the comparatively poor predicted pressures by the Boussinesq and Westergaard equations at shallow cover depths. First, the actual wheel loads are distributed over a finite area, approximated in design by the 10- by 20-in. (25.4- by 50.8-cm) rectangular AASHTO footprint. The Boussinesq and Westergaard equations predict the pressure beneath a concentrated load, resulting in a pressure that approaches infinity as the radial and vertical coordinates approach zero. For practical purposes, this means the theoretical equations should not be used to predict earth pressures in the immediate vicinity of the finite footprint, a limitation that has long been recognized. Also shown in Figure 4 is a pressure distribution calculated using the Boussinesq equation applied to a uniformly distributed pressure distributed over the tire contact areas. This curve, labeled "Boussinesq (distributed load)" in Figures 4-7, shows that the peak earth pressures predicted by this method are significantly less than the measured earth pressures. Second, the soil is neither linear elastic nor isotropic as is assumed in both theories. Some compensation for these differences is made by the parameters introduced in the regression analysis. Both the Boussinesq and the Westergaard theories were modified by changing variables from r and z to Br and Az, with factors A and B determined by regression to provide the best fit. In both cases, the data led to values for A and B different from 1.

The measured data may include random and systematic errors, characteristic of the transducers used. The physical

TABLE 2 RESULTS OF REGRESSION ANALYSIS

Equation No. (1)	Parameter (2)	Range Checked (3)	Value for Best Fit (4)	Ave. Error in psi (5)
(2a)	A	0.5-3.0	0.76	1.8
	B	0.5-3.0	1.50	
(2b)	A	0.5-3.0	0.61	1.4
	B	0.5-3.0	1.25	
(2c)	r_o	0.6-1.4 ft	0.62 ft	0.7
	z_o	0.6-1.4 ft	1.28 ft	
(2e)	A	0.5-3.6	3.0	45
	z_o	0.3-2.0 ft	1.2 ft	
(2f)	A	0.02-3.0	0.12	45
	z_o	0.5-8.0 ft	4.5 ft	
(2g)	A	0.02-3.0	0.1	50
	z_o	1-20 ft	12.5 ft	
(2h)	A	0.02-3.0	0.09	45
	z_o	1-20 ft	8.5 ft	

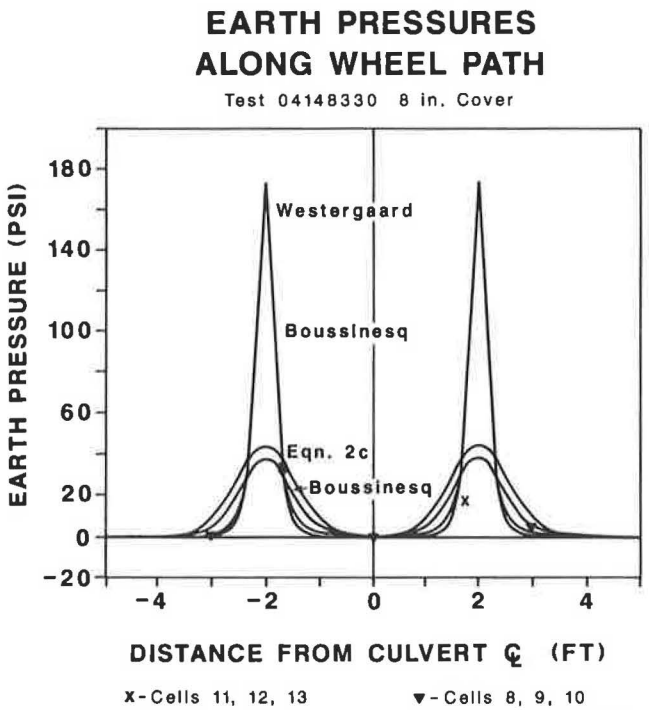

FIGURE 3 Comparison of empirical pressure prediction equations with data from Test 04148330.

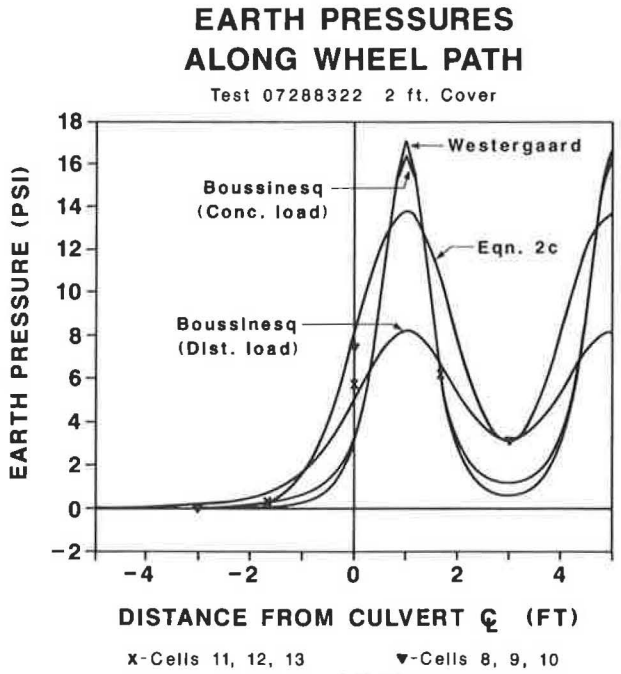

FIGURE 5 Comparison of empirical pressure prediction equations with data from Test 07288322.

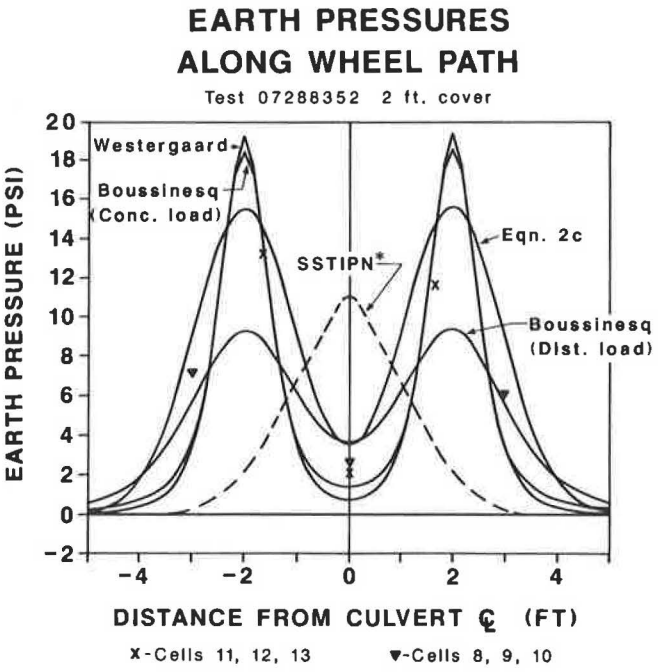

FIGURE 4 Comparison of empirical pressure prediction equations with data from Test 07288352.

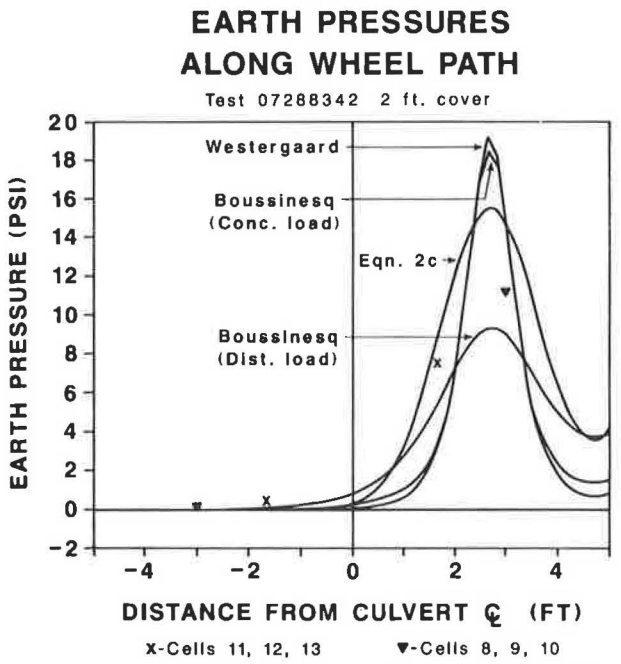

FIGURE 6 Comparison of empirical pressure prediction equations with data from Test 07288342.

size of the pressure cells results in an averaging of the earth pressure over an area approximately 6 in. (15.2 cm) square. Locally, high pressures caused by the wheel load may not be accurately reflected in the measured pressures, an effect that is more significant at shallow earth covers. This effect would result in indicated pressures less than actual pressures for cells located exactly at the point of maximum earth pressure, and indicated pressures more than actual pressures for cells located exactly at the point of minimum earth pressure. The measured earth pressures are typically several inches from local maximum theoretical pressures, at which points the errors due to the size of the transducer are expected to be negligible. Several data points lie at the location of theoretical minimum pressure, and the actual earth pressure may be slightly less than the indicated pressure at such points. Because the earth pressure gradients are not as great near the

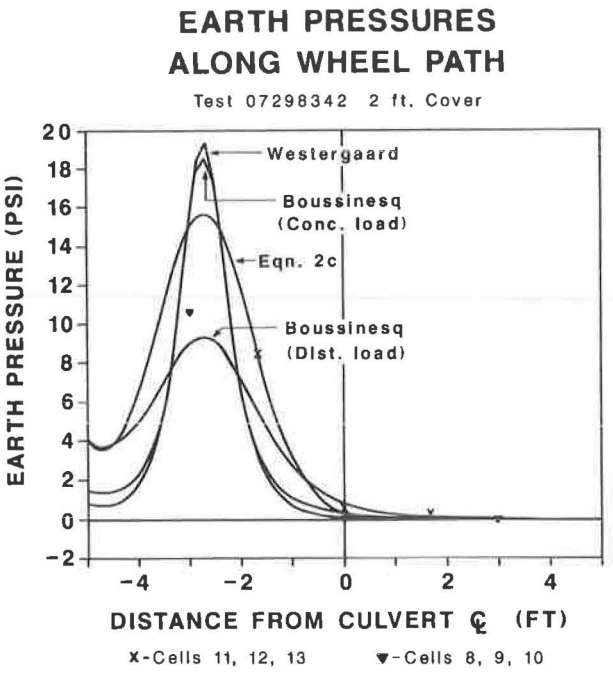

FIGURE 7 Comparison of empirical pressure prediction equations with data from Test 07298342.

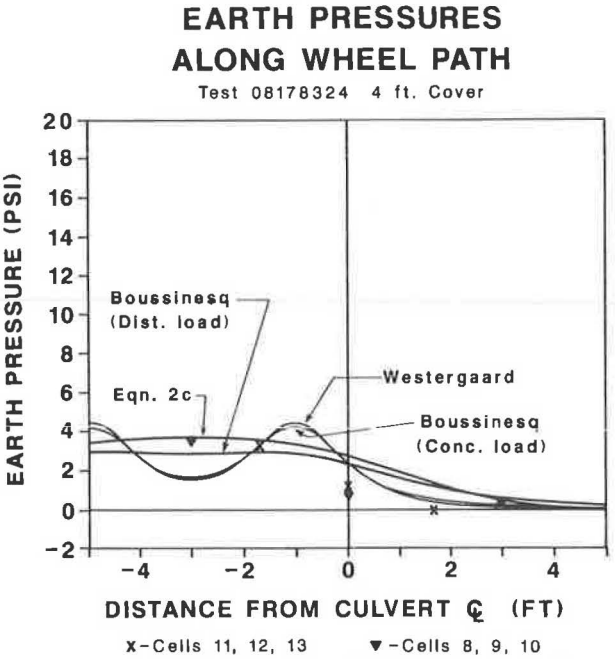

FIGURE 9 Comparison of empirical pressure prediction equations with data from Test 08178324.

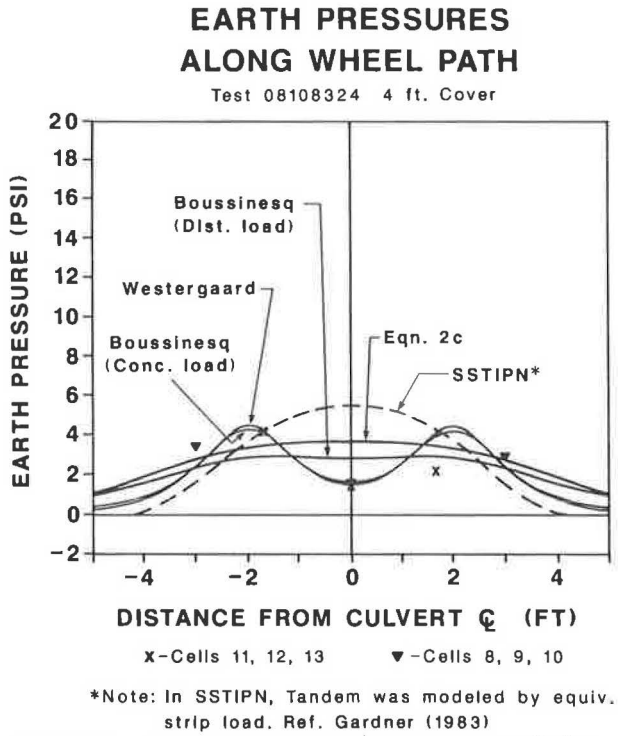

FIGURE 8 Comparison of empirical pressure prediction equations with data from Test 08108324.

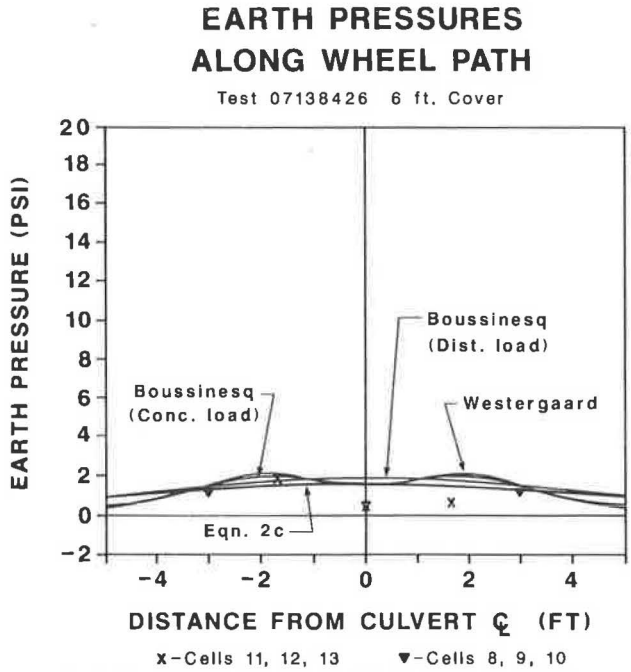

FIGURE 10 Comparison of empirical pressure prediction equations with data from Test 07138426.

local minimums, this systematic error is not as important near the minimum theoretical pressures as near the maximum theoretical pressures.

Hvorslev (*12*) discusses the effect of eccentricity of loading on a pressure cell. The presence of earth pressure gradients is equivalent to an eccentric loading because the center of pressure does not coincide with the geometric center of the cell. For a 6-in. (15.2-cm) diameter cell, Hvorslev (*12*) reports an average error of 7 percent underregistration for a 33 percent earth pressure variation across the face of the cell. For some of the extreme cases of shallow covers reported here, the pressure may experience variations on the order of 100 percent across the face of the cell. The result is that even in regions of uniform pressure gradient without the complicating factor of local pressure maxima, the pressure readings may include a systematic error, perhaps underregistering on the order of 20 percent.

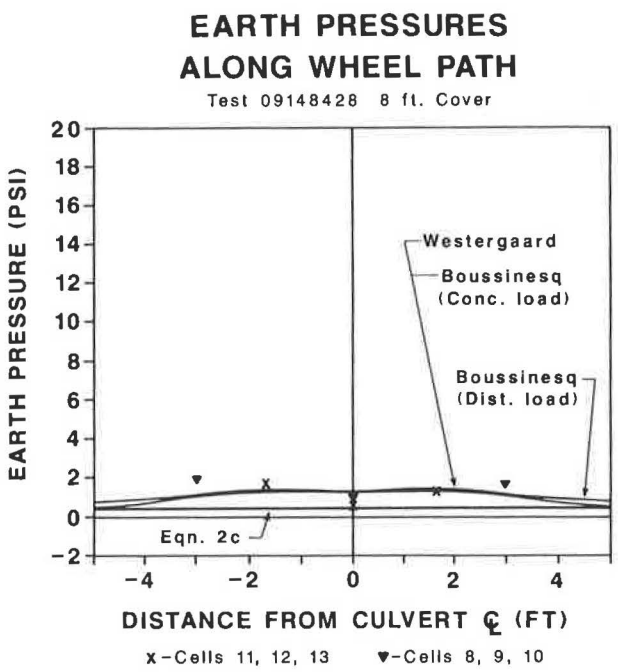

FIGURE 11 Comparison of empirical pressure prediction equations with data from Test 09148428.

Hvorslev (*12*) also discusses the effect of incomplete embedment of the pressure cell in the concrete slab. The cells were placed in the plastic concrete of the top slab as nearly flush as possible with the top surface. In spite of installation difficulties, protrusions of the cells were generally less than 0.25 in. (0.64 cm). Hence, any error caused by protrusion was expected to be underregistration in an amount dependent on the cell-soil modular ratio.

CONCLUSIONS

Data for measured live-load earth pressures is compared to existing theoretical and numerical methods, and to proposed empirical equations for predicting live-load earth pressures. The theoretical equations due to Boussinesq and Westergaard can be modified to satisfactorily model the measured earth pressure data when the depth of fill is 4 ft (1.22 m) or greater. For measured data at depths of cover up to 2 ft (1.22 m), the theoretical equations, even with empirical scaling parameters chosen for best fit, do not fit the data satisfactorily. The empirically determined Equation 2c appears to fit the data much better, particularly with respect to prediction of maximum earth pressure. The Boussinesq and Westergaard theoretical earth pressure equations for concentrated loads predict earth pressures considerably greater than the tire pressure at 8 in. (20.3 cm) of earth cover, whereas the Boussinesq equation applied to a uniformly distributed AASHTO footprint loading predicts pressures significantly less than measured. The potential systematic errors discussed probably result in underregistration of maximum earth pressures, and the suggested empirical equation appears to generally overestimate the measured earth pressures for covers up to 2 ft (0.61 m). Because the regression parameters in the proposed empirical equation are determined based on a data set including cover depths up to 8 ft (2.44 m), a better fit of the measured data for covers of 2 ft (0.61 m) or less could be determined. However, the apparent conservativism of the proposed equation is considered advantageous in the light of the potential systematic measurement errors.

The predicted wheel-load-induced pressures can be compared to the uniform pressures used in the AASHTO design procedure. Table 3 provides a comparison of the peak pressures calculated by Equation 2c and the AASHTO uniform design pressure for the 12-kip (53-kN) wheel loads of the test. Impact has not been included, and the 9.33-ft (2.84-m) width of the culvert top slab has been used as the limiting width of the AASHTO design area. From Table 3, it can be shown that the proposed equation predicts considerable higher pressures at 2 ft (0.61 m) of cover than does the AASHTO method. The deviation of the two methods is considerably less at greater depths of cover.

The proposed empirical equation offers the advantages of simplicity and accuracy for prediction pressures at cover depths of 2 ft (0.61 m) of less, with deviations from measured pressures generally resulting in conservative designs. It should be noted that the proposed equation does not provide a different pressure distribution transverse to traffic, as would be expected because of the shape of the wheel footprints.

The finite element solution compares acceptably with the measured data at depths of fill of 4 ft (1.22 m) (*13*), but at shallow covers of 2 ft (0.61 m) or less the finite element model resulted in unconservative predicted pressures. The finite element method is a two-dimensional solution, and direct comparison with the three-dimensional measured and theoretical earth pressures is difficult. In addition, the finite element solution used a single axle carrying 32 kip (142 kN) instead of the actual tandem 24-kip (107-kN) axles tested. The finite element simulation was made in advance of the tests, using soils data from laboratory tests at the site and proven modeling techniques.

TABLE 3 COMPARISON OF PEAK EARTH PRESSURES TO AASHTO METHOD

Cover (ft)	AASHTO Pressure (psi)	Equation (2c) Pressure (psi)
0.67	---	40
2	6.8	15.6
4	2.7	3.6
6	2.1	1.6
8	1.8	0.5

Note: Impact is neglected.

PRACTICAL APPLICATIONS

The measured data are applicable to designers of box culverts for service under less than approximately 2 ft (0.61 m) of cover. Extension of the results to box geometries or soils significantly different from those tested should be done with caution. The data or the empirical equations presented can be used for design or as a test case for evaluation of finite element methods to soil-structure interaction for culverts or similar structures.

ACKNOWLEDGMENTS

The research was funded by the Texas State Department of Highways and Public Transportation, to whom the authors are grateful. Other researchers contributing substantially included Harry M. Coyle, Richard E. Bartoskewitz, and Robert L. Lytton. The assistance and encouragement of the TSDHPT personnel, particularly Charles Terry, is appreciated. Assistance with construction and instrumentation by the Construction Equipment Training Division and the Texas Transportation Institute Instrument Shop is acknowledged.

REFERENCES

1. *Standard Specifications for Highway Bridges*. 13th ed., AASHTO, Washington, D.C., 1983.
2. N. M. Newmark. *Influence Charts for Computation of Stresses in Elastic Foundations*. Bulletin 338. University of Illinois Engineering Experiment Station, 1942 (reprinted June 1964).
3. L. Jurgenson. The Application of Theories of Elasticity and Plasticity to Foundation Problems. *Journal of the Boston Society of Civil Engineers*, July 1954.
4. E. J. Yoder and M. W. Witczak. *Principles of Pavement Design*. 2nd ed., Wiley, New York, 1975, 711 pp.
5. *Design Manual: Soil Mechanics, Foundations, and Earth Structures*. DM-7, NAFAC, Department of the Navy, 1971, 223 pp.
6. M. G. Katona and J. M. Smith. *CANDE: User Manual*. FHWA, U.S. Department of Transportation, Oct. 1976.
7. S. C. Anand. Stress Distributions Around Shallow Buried Rigid Pipes. *Journal of the Structural Division, ASCE*, Vol. 100, No. ST1, Proc. Paper 10258. Jan. 1974, pp. 161-174.
8. T. Krauthammer. Shallow-Buried RC Box-Type Structures. *Journal of the Structural Division, ASCE*, Vol. 110, No. 3, March 1984, pp. 637-651.
9. R. W. James, D. E. Brown, R. E. Bartoskewitz, and H. M. Coyle. *Earth Pressures on Reinforced Concrete Box Culverts*. Research Report 294-2F. Texas Transportation Institute, Texas A&M University System, College Station, Aug. 1985.
10. G. B. Sowers and G. F. Sowers. *Introduction to Soil Mechanics and Foundations*. 3rd ed. Macmillan, New York, 1970.
11. H. M. Westergaard. *A Problem of Elasticity Suggested by a Problem of Soil Mechanics: Soft Material Reinforced by Numerous Strong Horizontal Sheets*. Contributions to the Mechanics of Solids. Macmillan, New York, 1938.
12. M. J. Hvorslev. *The Changeable Interaction Between Soils and Pressure Cells; Tests and Reviews at the Waterways Experiment Station*. Technical Report S-76-7. Soils and Pavements Laboratory, U.S. Army Engineer Waterways Experiment Station. Vicksburg, Miss., June 1976.
13. M. P. Gardner, J. K. Jeyapalan, and R. W. James. *The Behavior of Reinforced Concrete Box Culverts Under Symmetrical and Unsymmetrical Live Loads*. Research Report 326-2F, Texas Transportation Institute, Texas A&M University System, College Station, Sept. 1983 (revised Aug. 1985), 161 pp.